

Comparative Study of the Adsorption Mechanism and Photochemical Oxidation of Chlorophenols on a TiO₂ Nanocatalyst

Muneer M. Ba-Abbad^{1, 2*}, Abdul Amir H. Kadhum¹, Abu Bakar Mohamad¹, Mohd S. Takriff¹,
Ramzi T. T. Jalgham¹

¹ Department of Chemical and Process Engineering, Faculty of Engineering and Built Environment, Universiti Kebangsaan Malaysia, 43600, Bangi, Selangor, Malaysia

² Department of Chemical Engineering, Faculty of Engineering and Petroleum, Hadhramout University of Science & Technology, Mukalla, Hadhramout, Yemen

*E-mail: muneer711@gmail.com

Received: 30 July 2012 / Accepted: 24 September 2012 / Published: 1 November 2012

The anatase structure of titanium dioxide (TiO₂) nanoparticles was prepared via sol-gel technique and investigated by X-ray diffraction (XRD). The activity of TiO₂ was evaluated by photocatalytic degradation of chlorophenolic compounds namely 2-chlorophenol (CP), 2,4-dichlorophenol (DCP) and 2,4,6-trichlorophenol (TCP) under solar radiation. A computational technique based on semiempirical and density functional theory (DFT) was used to study the effects of chlorophenolic compounds adsorption on the anatase TiO₂ (100) surface. Then, E_{HOMO} , E_{LUMO} and ΔE were evaluated by three methods, each of which uses density functional theory (DFT) with semiempirical methods. A molecular dynamics (MD) simulation was employed to obtain a great understanding of the adsorption behavior of chlorophenolic compounds on the anatase TiO₂ (100) surface. The results of the CP and DCP molecules revealed a perpendicular adsorption via chloride with the surface lattice titanium ion, while this behavior was changed to planar for TCP. To make a comparison between experimental and theoretical calculations, the adsorption energies of chlorophenolic molecules were found to be increased in the order TCP < DCP < CP, as confirmed with the photocatalytic degradation efficiency from the experimental data.

Keywords: Adsorption energy, molecular dynamics, chlorophenolic, TiO₂, degradation.

1. INTRODUCTION

In the last decade, a TiO₂ nanoparticle has been used for most goals related to the photocatalytic degradation of chlorinated compounds, because these nanoparticles are nontoxic, highly

efficient, and inexpensive and chemically stable. Moreover, the energy band gap is 3.2 eV for the anatase and 3.0 eV for the rutile phase [1-3]. Anatase and rutile are two phases that have been used in many applications, such as photocatalysts[4]. The anatase phase reported has a higher photocatalytic activity than the rutile phase [5]. The lattice planes of anatase particles consist of (1 0 1), (1 0 0) and (0 0 1) and the structure of anatase was observed to be affected because of the methods preparation and the experimental conditions [6,7]. According to previous studies, the stability of anatase (1 0 1) and (0 0 1) surface planes is slightly more than that of the plane (100) [8]. The photocatalytic degradation of chlorinated compounds on TiO₂ has been influenced by the adsorption process [9]. The changes to or substitutions of some groups on the aromatic ring affects the degree of adsorption and the properties of the adsorbed molecules [10]. Previous studies have indicated that the degradation of organic compounds occurs on a photocatalytic surface, which indicates that the adsorption of an organic molecule is the main factor in evaluating the rate of a photocatalytic reaction [11-14]. Palmisano et al. [15], focused on the oxidation of phenylamine using TiO₂ as a photocatalyst and noted that the adsorption of the molecules onto the TiO₂ surface is a relevant factor for the degradation process. Perpendicular adsorption of the benzene ring and of 4-chlorophenol molecules has been reported on TiO₂ surfaces [16-18]. In computational chemistry, semiempirical and density functional theory (DFT) methods have been used for large nanoparticles with hundreds to thousands of atoms and for long time scale molecular dynamics simulations [19]. The objectives of this study were to evaluate the photocatalytic degradation of the chlorophenolic compounds, CP, DCP and TCP by TiO₂ nanoparticles as photocatalysts and to investigate the relationship between quantum chemical calculations (adsorption energy) and the photocatalytic degradation efficiency using Quantum chemical (Q.C) and Monte Carlo (M.C) techniques.

2. EXPERIMENTS

TiO₂ nanoparticles were synthesized by hydrolyzing titanium tetra isopropoxide (TTIP) in the presence of an ethanol and water mixture. Additionally, all of the characterization and optical properties of TiO₂ nanoparticles were reported [20]. Photodegradation experiments of chlorophenols were conducted in a slurry batch reactor. All of the experiments were conducted under the optimal conditions on sunny days at times between 11.00 a.m. and 2.30 p.m. using 100 ml of solution containing 50 mg l⁻¹ chlorophenols with 2 g l⁻¹ of TiO₂ nanoparticles, as reported elsewhere [20]. The degradation of chlorophenols was determined using an Agilent 1200 HPLC platform with a Jones LC-18 column (250 mm x 4.6 mm x 4 μm), and a variable wavelength UV detector. A 20:80 ratio of acetonitrile to water v/v with 0.01 M phosphoric acid (H₃PO₄) as a mobile phase and a flow rate of 1.0 ml min⁻¹ were applied. Then, 20 μL of photolyzed sample was subjected to HPLC analysis and the determination of CP, DCP and TCP was conducted using detector wavelength of 254, 284 and 293 nm, respectively. For the mixed chlorophenols, 100 ml of the mixture was run under the same experimental conditions, and an analysis by HPLC at a wavelength of 280 nm was applied for detection [21].

3. THEORETICAL ANALYSIS

An electrostatic structures test of the chlorophenolic compounds was performed and is described in this section. We investigated whether there was relationship between the photocatalytic degradation efficiency of the chlorophenolic compounds and their quantum chemical parameters. The mechanism of chlorophenole adsorption on a photocatalyst surface was studied using Quantum Chemical (Q.C) and Monte Carlo (M.C) approaches with the Material Studio (M.S) version 5.5 software, which was developed and distributed by Accelrys. The structures of chlorophenolic compounds are given in Fig.1. The quantum chemical calculations were evaluated using three methods of Density function theory (DFT) namely, the Becke exchange plus Lee-Yang-Parr correlation (BLYP), Perdew-Burke-Ernzerhof correlation (PBE) and the Becke exchange plus Perdew PB correlation, as well as three methods with semiempirical approaches (AM1, PM3 and PM6) [22].

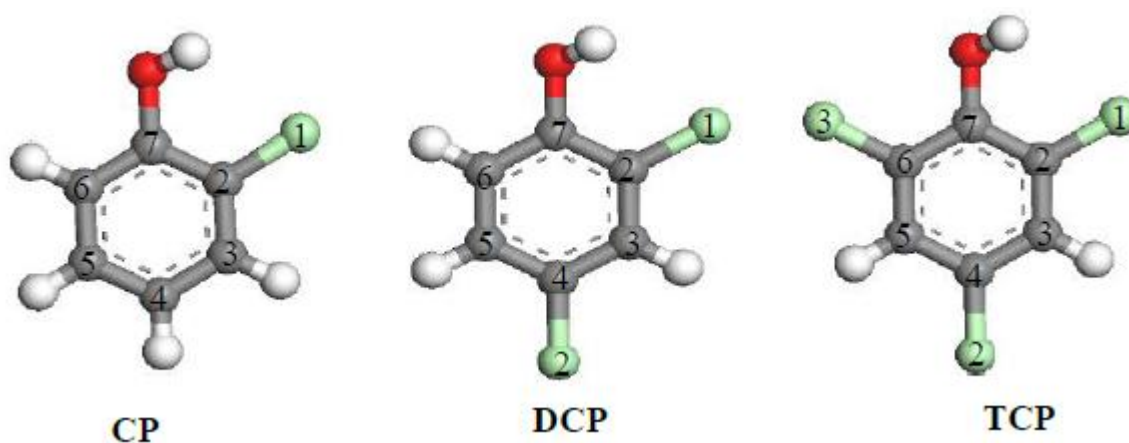


Figure 1. Structure of chlorophenolic compounds, gray spheres(C); white spheres (H); red spheres (O) and green spheres (Cl).

Fukui functions are qualitative ways of measuring and displaying the reactivity of regions of a molecule with respect to electrophilic and nucleophilic attacks to the charge density. The Fukui index was also analyzed to obtain detailed information about the local reactivity. The Fukui function (f_k) is defined as the first derivative of the electronic density $\rho(\vec{r})$ with respect to the number of electrons N in a constant external potential $v(\vec{r})$ as given in Eq.1[23].

$$f_k = \left(\frac{\partial \rho(\vec{r})}{\partial N} \right)_{v(\vec{r})} \quad (1)$$

$$f_k = \left(\frac{\partial \rho(\vec{r})}{\partial N} \right)_{v(\vec{r})}$$

Applying a finite differences approximation, the Fukui function can be written for nucleophilic and electrophilic attacks, respectively, as given in Eqs. 2 and 3

$$f_k^+ = q_k(N + 1) - q_k(N) \quad (2)$$

$$f_k^- = q_k(N) - q_k(N - 1) \quad (3)$$

where $q_k(N + 1)$, $q_k(N)$, and $q_k(N - 1)$ are defined as the atomic charges of the anionic, neutral and cationic species, respectively. The Fukui functions were obtained through the finite difference approximation using the Hirshfeld and Mulliken population analysis [23]. Understanding adsorption phenomena is of key importance in photocatalytic degradation processes. A Monte Carlo simulations (M.C) technique incorporating molecular mechanics and molecular dynamics was applied to study adsorption phenomena. Monte Carlo simulations can help to indicate the most stable adsorption sites on metal surfaces and to investigate the preferential adsorption of mixture components [24]. The negative values of adsorption energies were from the stabilization of adsorption of the chlorophenols-TiO₂ system [25].

4. RESULTS AND DISCUSSION

4.1. Experimental results

The phase composition and the crystallite size of the prepared TiO₂ samples were evaluated by XRD analysis. The XRD patterns of TiO₂ powder calcinated at 500 °C is shown in Fig. 2. The peaks obtained at various 2θ were identified in comparison with JCPDS-84-1286, and it was confirmed that the particles are crystalline with an anatase structure ($2\theta=25.4^\circ$). It is noteworthy that the diffractograms of the samples do not present any peak assigned to the rutile phase ($2\theta= 27.36$). The average crystal size, band gap and surface area of the TiO₂ nano-particles were 19 nm, 3.11 eV and 34.47 m²/g, respectively.

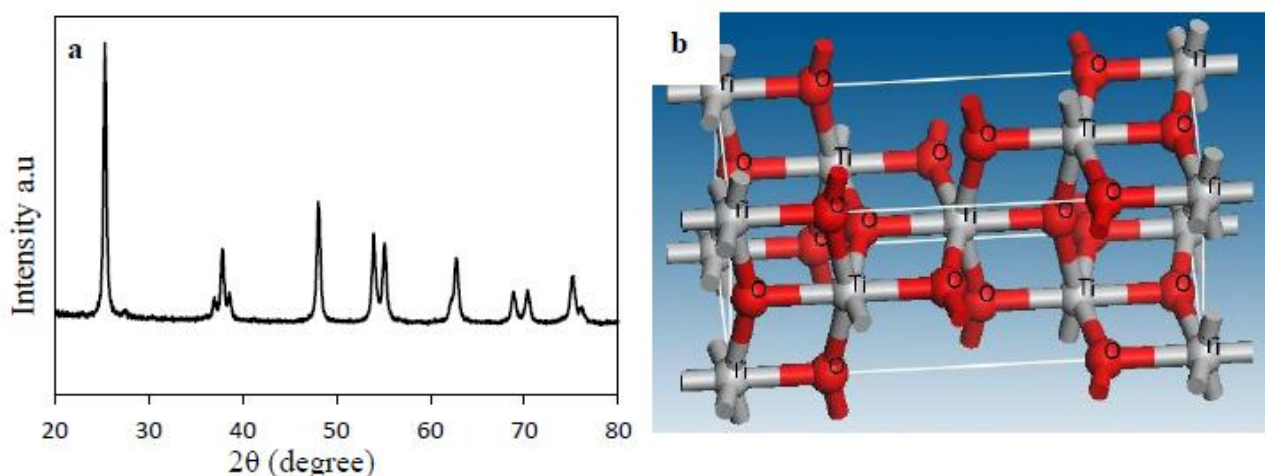


Figure 2. (a) X-ray diffraction patterns of TiO₂ anatase, (b) structure of anatase phase, red spheres (O) and gray spheres (Ti).

The photodegradation of CP, DCP and TCP under solar irradiation in the presence of TiO₂ nanoparticles was investigated. The values of degradation efficiencies are listed in Table 1. The experimental results on degradation show that the efficiency decreases gradually from CP to TCP. This result indicates that, when the chlorine functional group in the phenol ring was increased, the efficiency of the degradation was decreased. Further explanation of the behavior of chlorophenole degradation will be discussed in the theoretical section. Similarly, the experimental results on the same sequence of degradation on heterogeneous catalysts were reported [26].

Table 1. Photocatalytic degradation efficiency of chlorophenols using TiO₂ nano-particles

Molecule	Concentration (mg/l)	Catalyst loading (g/l)	Time of irradiation (min)	Degradation Efficiency (%)
CP	50	2	60	95
DCP	50	2	60	93
TCP	50	2	60	75

The sequence of chlorophenols degradation was investigated by mixing it with the same concentration of 50 mg l⁻¹ and experimental conditions. The experimental results obtained for the degradation indicated a total removal of CP in less than 30 min. The HPLC result of the DCP shows decreasing with irradiation time increased because almost all of the TCP was converted into DCP, as shown in Fig.3.

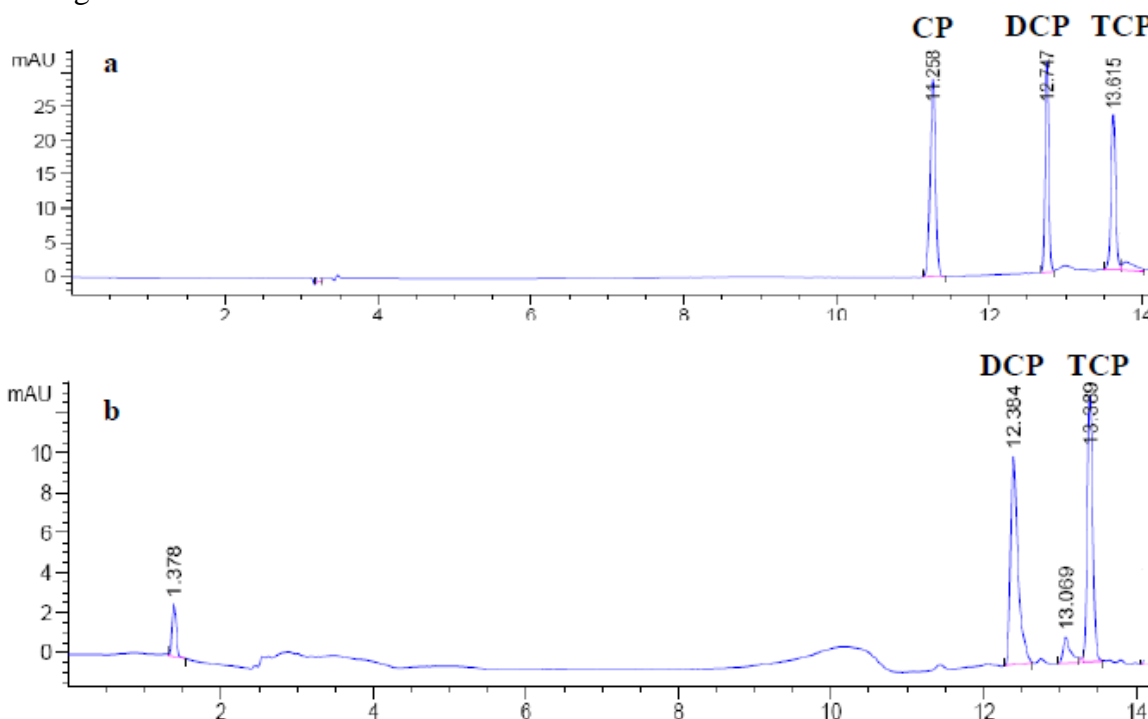


Figure 3. The HPLC results of chlorophenols mixture degradation at different time (a) 0 min (b) 30 min.

Fast degradation of CP molecules was observed, when the DCP converted into CP within the degradation process. Accordingly, no CP peak appeared in the HPLC results, which indicated the highest degradation of CP. These results show that the degradation of the chlorophenol mixture uses the same sequence when it is individual as reported in Table 1.

4.2. Theoretical results

4.2.1 Quantum chemical calculations

The quantum chemical methods (i.e., density functional theory and semiempirical) are all based on solving the time independent Schrödinger equation for the electrons of a molecular system as a function of the positions of the nuclei [27, 28]. The premise behind the density functional theory is that the energy of a molecule can be determined from the electron density instead of from a wave function [29, 30]. Based on the frontier orbital theory, the reaction of the reactants occurred mainly on the highest occupied molecular orbital (HOMO) and the lowest unoccupied molecular orbital (LUMO) [31, 32]. Therefore, the frontier orbital theory was used to determine possible modes of interaction between the molecules and the metal. It is necessary to investigate the distribution of HOMO and LUMO for an exploration of the degradation mechanism. The optimized structure of the chlorophenolic molecules and the distribution of HOMO and LUMO using BLYP and PM6 as an example of density functional theory and semiempirical methods are presented in Figs. 4 and 5, respectively.

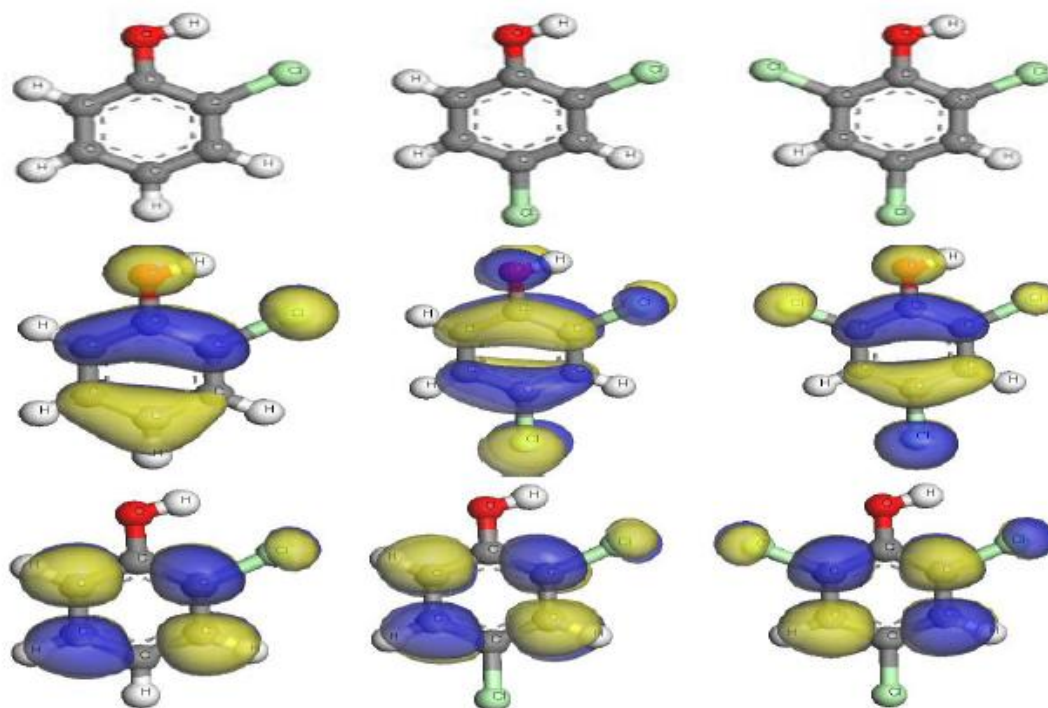


Figure 4. The frontier molecule orbital density distributions of CP, DCP and TCP: a HOMO and b LUMO using BLYP, DFT method.

Based on DFT and the semiempirical results, the molecules have similar frontier orbital distributions on the Cl and the O atoms, as well as in the phenol ring. The density HOMO distribution on the Cl and O atoms decreased when the hydrogen atom was replaced with a Cl atom.

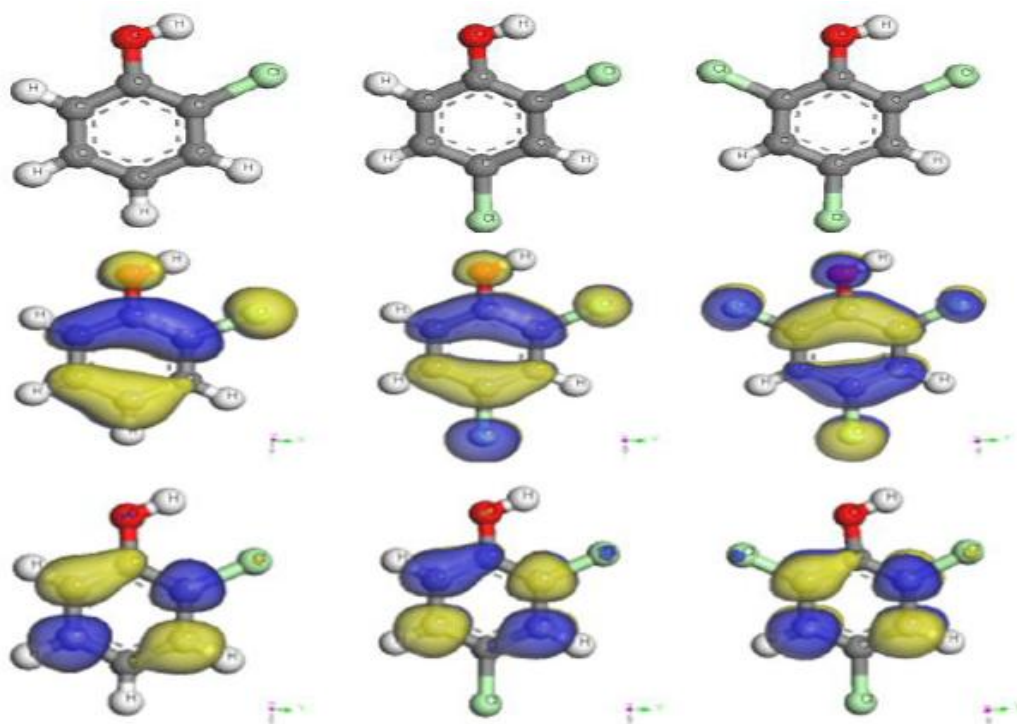


Figure 5. The frontier molecule orbital density distributions of CP, DCP and TCP: a HOMO and b LUMO using PM6, Semi empirical method.

Table 2. Orbital energies calculation for chlorophenolic molecules using DFT method

Method	Molecule	E_{HOMO} (eV)	E_{LUMO} (eV)	ΔE (eV)
BLYP	CP	-5.36	-1.09	-4.27
	DCP	-5.41	-1.44	-3.97
	TCP	-5.57	-1.67	-3.90
BBE	CP	-5.51	-1.22	-4.28
	DCP	-5.53	-1.57	-3.96
	TCP	-5.68	-1.79	-3.89
PB	CP	-5.50	-1.21	-4.29
	DCP	-5.53	-1.56	-3.98
	TCP	-5.69	-1.79	-3.90

E_{HOMO} is often associated with the electron-donating ability of the molecule, which indicates the ability of the molecule to accept electrons. Therefore, high values of E_{HOMO} are likely to indicate a tendency of the molecule to donate electrons to the appropriate acceptor molecules with low energy. The lower values of E_{LUMO} indicate a higher probability that a molecule accepts electrons [33].

Moreover, the gap ΔE between the HOMO and LUMO energy levels of the molecules ($\Delta E = E_{HOMO} - E_{LUMO}$) is another important factor that should be accounted for with respect to the molecule's abilities. The values of E_{HOMO} , E_{LUMO} and ΔE for chlorophenolic molecules are listed in Tables 2 and 3.

Table 3. Orbital energies calculation for chlorophenolic molecules using Semi empirical method.

Method	Molecule	E_{HOMO} (eV)	E_{LUMO} (eV)	ΔE (eV)
AM1	CP	-9.26	0.03	-9.29
	DCP	-9.27	-0.24	-9.03
	TCP	-9.39	-0.50	-8.89
PM3	CP	-9.19	-0.22	-8.97
	DCP	-9.41	-0.58	-8.82
	TCP	-9.63	-0.90	-8.73
PM6	CP	-9.24	-0.27	-8.97
	DCP	-9.26	-0.65	-8.61
	TCP	-9.36	-0.94	-8.42

The values of ΔE ($E_{HOMO} - E_{LUMO}$) that were calculated based on six methods show a decrease from the CP to TCP. Additionally, the Fukui was calculated based on Mulliken and Hirshfeld, and the values are given in Table 4 and 5. The largest Fukui indices were observed only on hetero atoms (Cl and O).

Table 4. Fukui index for chlorophenolic molecules calculated based on Mulliken

Molecule	atom	f_R^+	f_R^-
CP	O	0.05	0.146
	Cl ₁	0.156	0.177
DCP	O	0.049	0.125
	Cl ₁	0.151	0.147
	Cl ₂	0.13	0.227
TCP	O	0.043	0.119
	Cl ₁	0.147	0.129
	Cl ₂	0.157	0.156
	Cl ₃	0.123	0.21

The Fukui indices of hetero atoms based on Mulliken and Hirshfeld were observed to decrease with the addition a Cl atom, which means that chlorophenolic molecules have a higher capability for donating and accepting electrons [34]. The Fukui value of the Cl atom in all of the chlorophenols is high than that of oxygen, which indicates a higher site reactivity in the molecules. This result supports the idea that the adsorption of chlorophenol by a Cl atom to the surface of TiO₂ has occurred. The CP and DCP molecules adsorbed by Cl as active sites were observed, which determines that the geometry

of the adsorption as is perpendicular. When the Cl increases in the phenol ring by more than two, as in TCP, the geometry of adsorption is changed to parallel as shown in Fig.8. These results confirmed the degradation efficiency by experimental study, as presented in Table 1.

Table 5. Fukui index for chlorophenolic molecules calculated based on Hirshfeld

Molecule	atom	f_R^+	f_R^-
CP	O	0.052	0.142
	Cl ₁	0.141	0.156
DCP	O	0.05	0.123
	Cl ₁	0.137	0.128
	Cl ₂	0.108	0.205
TCP	O	0.044	0.116
	Cl ₁	0.134	0.11
	Cl ₂	0.140	0.135
	Cl ₃	0.102	0.189

Bond-dissociation energy is a term that is used to measure the bond strength, and it can be defined as the energy that is required to separate the individual atoms or to break the bond between two atoms. The bond strength (energy) can be directly related to the bond length/bond distance. In the present study, the length of the C-C, C=C, C-O, O-H and C-Cl bonds are measured after the chlorophenolic molecules are optimized, as shown in Fig. 6. The values of the bond lengths of all of the molecules are listed in Table 6. The length of the C-C, C=C, C-O and O-H bonds, show slight changes with an increasing number of Cl atoms in the molecule. Based on these results, the weakest bond of C-Cl is observed and can be easily broken because of the longer length bonds.

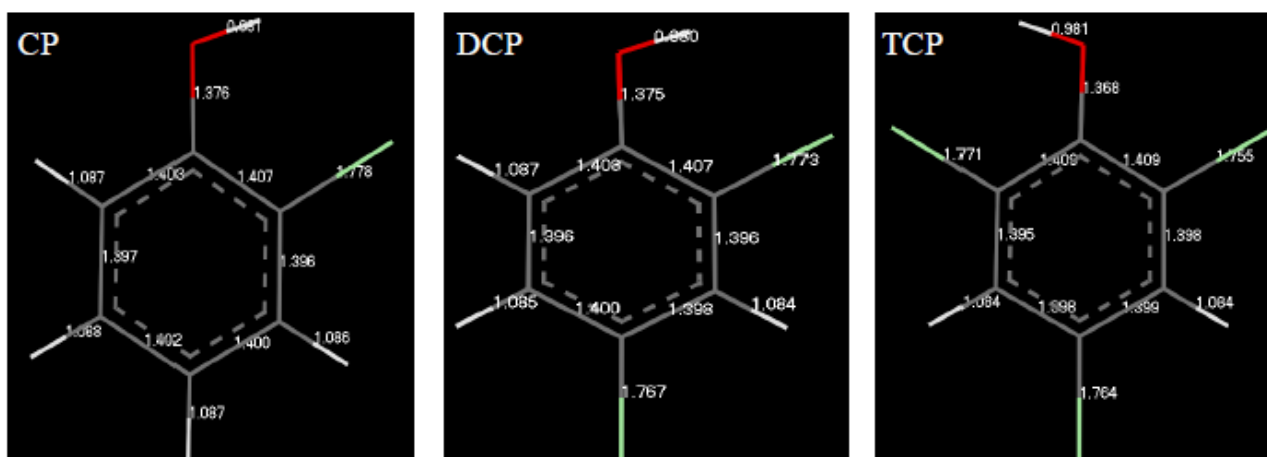


Figure 6. Bond length of chlorophenolic molecules

However, a larger change in the C-Cl bond was observed, especially in the ortho position substitution bond in the TCP molecule. The bond length of Cl₁-C₂ decreases from the CP to TCP, according to the data obtained. When the Cl atom substituent increased in the molecules, the length of the Cl₂-C₄ bond became shorter similar to both the DCP and TCP. In general, the C-Cl bond length decreased with the addition of a Cl atom in the phenol ring as reported in some previous studies [35-37]. The length of the C-Cl bond in chlorophenolic molecules decreased from the CP to TCP, as shown in Table 6. These values support the pattern of degradation of these compounds.

Table 6. Bond length of all chlorophenolic molecules after optimization

Bond identity of CP	Bond length, Å	Bond identity of DCP	Bond length, Å	Bond identity of TCP	Bond length, Å
Cl ₁ -C ₂	1.778	Cl ₁ -C ₂	1.773	Cl ₁ -C ₂	1.755
C ₂ =C ₃	1.396	C ₂ =C ₃	1.396	C ₂ =C ₃	1.398
C ₃ -C ₄	1.400	C ₃ -C ₄	1.398	C ₃ -C ₄	1.399
C ₄ =C ₅	1.402	Cl ₂ -C ₄	1.767	Cl ₂ -C ₄	1.764
C ₅ -C ₆	1.397	C ₄ =C ₅	1.400	C ₄ =C ₅	1.398
C ₆ =C ₇	1.403	C ₅ -C ₆	1.396	C ₅ -C ₆	1.395
C ₇ -C ₂	1.407	C ₆ =C ₇	1.403	Cl ₃ -C ₆	1.771
C ₇ -O	1.376	C ₇ -C ₂	1.407	C ₆ =C ₇	1.409
O-H	0.981	C ₇ -O	1.375	C ₇ -C ₂	1.409
		O-H	0.980	C ₇ -O	1.368
				O-H	0.981

4.2.2. Adsorption geometries

The optimized geometries of the adsorption simulation of the chlorophenolic molecules on the TiO₂ surface at equilibrium are presented in Fig. 7. It can be observed that the CP orients itself approximately perpendicularly to the surface, with the chloro (Cl) and OH substituents pointing down onto the surface of the TiO₂, Hilal et al. [18] have reported perpendicular adsorption of *p*-chlorophenol molecules on the surface of the TiO₂ catalyst via hydrogen bonding. At same time, some studies have noted different results for the degradation of 4-chlorophenol compared with simulation calculations [38,39]. Accordingly, the simulation finding confirms that the perpendicular adsorption geometry is very important to the degradation of chlorophenols on the surface of the catalyst. However, the DCP is also adsorbed perpendicularly to the surface of the TiO₂. The adsorption of the DCP is affected by the addition of a Cl atom, which is slightly different compared to the CP. From these observations, the adsorption of chlorophenols on the surface of the TiO₂ via Cl atoms especially in the DCP could perhaps be attributed to increases in the electronegativity of the Cl atom in the phenol ring. There is no study to date about the adsorption of phenol molecules containing multiple or single Cl atoms besides the OH group, in the ortho position compared to the para position. Additionally, like the CP and DCP, the TCP is oriented differently is parallel adsorbed to the surface of TiO₂. This observation could be because the active Cl atoms were distributed equally throughout the surface of the TCP molecule. The

adsorbed oxygen works as a trap to generate an electron in the conduction band as has been reported for a system of heterogeneous photocatalytic reactions [40].

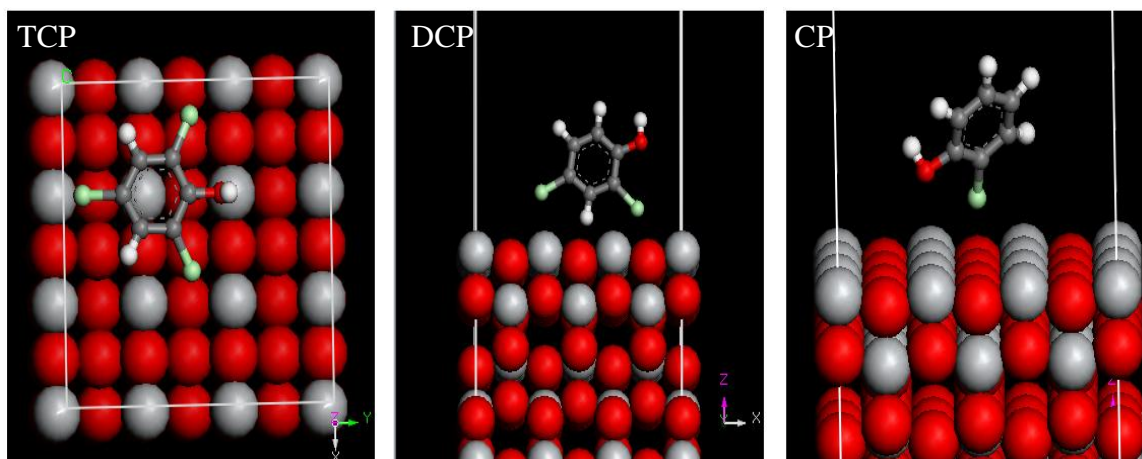


Figure 7. Equilibrium configuration performance of chlorophenolic molecules on TiO_2 surface.

Highly reactive oxygen superoxide $\cdot\text{O}_2^-$ will attack the C in chlorophenols, which hold the Cl atom, as reported by Hilal et al [18], whereas, X. Li et al. [38] have noted that the superoxide $\cdot\text{O}_2^-$ attacks the C, that is linked to the OH group. These results indicated that the position of Cl play an important role in this study. According to the simulation findings, the experimental results followed along the same lines for the degradation sequence of the CP, DCP and TCP. To our knowledge no previous theoretical studies are available regarding adsorption of Cl atoms located at different positions of the phenol molecule at the surface of TiO_2 .

4.2.3 Adsorption energy calculations

The relationship between adsorption and photocatalytic degradation has been reported by several authors [41,42]. Therefore, the adsorption factor of organic compounds is an important factor in the enhancement of the oxidation process [43]. A Monte Carlo simulation was performed to study the adsorption behavior of the chlorophenolic molecules on the TiO_2 surface. Fig. 8 shows the energy distribution curves for the simulated systems, including the TiO_2 surface and the chlorophenolic molecules.

The rigid adsorption energy, the deformation energy and the adsorption energy were released, when the adsorbate components (chlorophenolic molecules) were adsorbed on the metal surface. All of the rigid adsorption, the deformation and the adsorption energies were evaluated by Monte Carlo simulation and reported in Table 7. An important energy for the degradation of chlorophenolic compounds on the TiO_2 surface was the adsorption energy from the first step of the degradation process. The adsorption energy (E_{ads}) values revealed high energy for the chlorophenolic molecules

toward the TiO₂ surface. All of the values of E_{ads} were negative, which indicates that the adsorption could occur spontaneously.

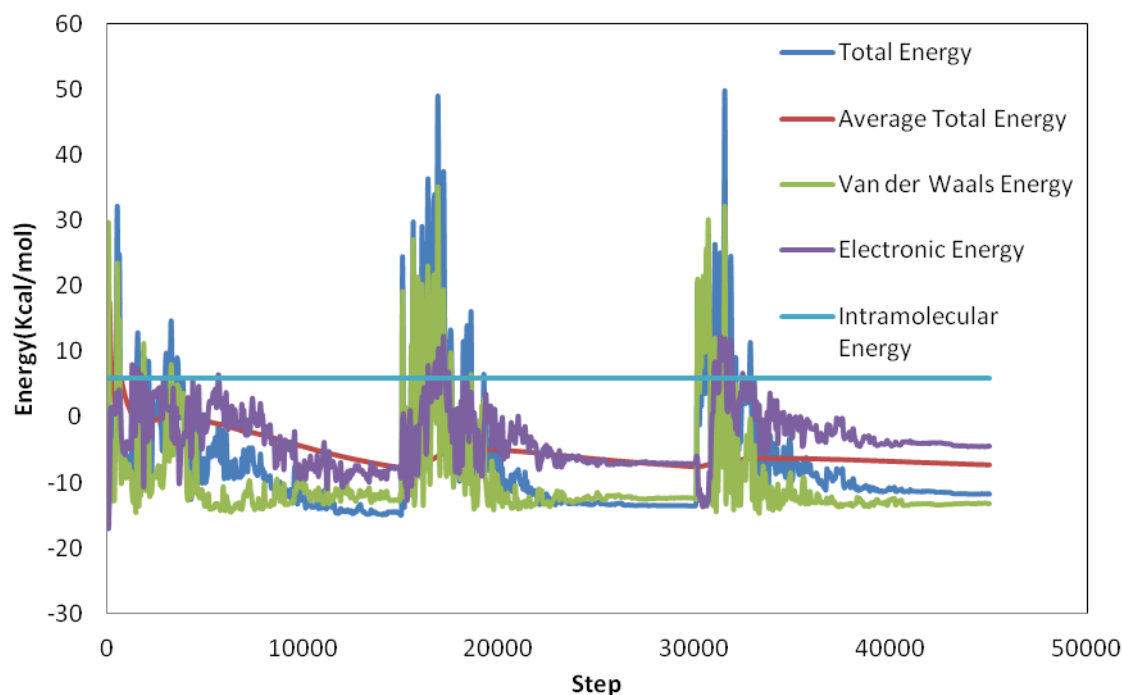


Figure 8. Energy distribution curves for chlorophenolic on surface TiO₂

The adsorption energy of chlorophenolic molecules increased in the following order TCP < DCP < CP. High values of E_{ads} indicate that the chlorophenolic molecules with the highest degradation efficiency are in concordance with the experimental measurements that were found.

Table 7. The energies calculated using the Monte Carlo simulation for adsorption chlorophenolic molecules on TiO₂ surface.

Molecule	Rigid adsorption energy	Deformation energy	Adsorption energy
CP	-84.07	9.66	-74.41
DCP	-76.13	4.55	-71.58
TCP	-79.84	12.08	-67.76

5. CONCLUSION

Chlorophenolic compounds showed different adsorption energies of molecules on the surface of TiO₂ nanoparticles through quantum chemical calculations (i.e., density functional theory (DFT)

and semi empirical). The values of E_{HOMO} , E_{LUMO} , ΔE and the Fukui indices were found on the Cl and O atoms to be the largest values in chlorophenolic molecules. The optimization of the adsorption geometry of the CP and DCP molecules were found to be perpendicular and parallel for the TCP, which confirms the linkage of the CP, DCP and TCP molecules to the TiO_2 surface via Cl atoms on the chlorinated compounds. The results for the adsorption energies from the simulations in this study showed the same experimental degradation sequence. The adsorption energies were found to -74.41, -71.58 and -67.76 for the CP, DCP and TCP, respectively. These results were in concordance with the photocatalytic degradation efficiencies of the CP, DCP and TCP, which were 95 %, 93 % and 75 %, respectively.

ACKNOWLEDGEMENTS

The authors are thankful to the Universiti Kebangsaan Malaysia (UKM-DLP-2011-064) and Hadhramout University of Science and Technology, Yemen for their financial support.

References

1. S. Song, C. Wang, F. Hong, Z. He, Q. Cai, *Appl. Surf. Sci.*, 257 (2011) 3427.
2. C. Lettmann, K. Hildenbrand, H. Kisch, W. Macyk, W. Maier, *Appl. Catal.*, B, 32(2001) 215.
3. I. B. Obot and N.O. Obi-Egbedi, *Corros. Sci.*, 52 (2010.) 657.
4. V.E. Henrich and P.A. Cox, *The Surface Science of Metal Oxides*, Cambridge University Press, Cambridge (1996).
5. A. Sclafani and J. M. Herrmann, *J. Phys. Chem.*, 100 (1996) 13655.
6. A. Vittadini, A. Selloni, F.P. Rotzinger, M. Gratzel, *Phys. Rev. Lett.*, 81 (1998) 2954.
7. Y. Gao and S. A. Elder, *Mater. Lett.*, 44(2000) 228.
8. G.S. Herman and Y. Gao, *Thin Solid Films*, 397(2001) 157.
9. D. Robert, S. Parra, C. Pulgarin, A. Krzton, J.V. Weber, *Appl. Surf. Sci.*, 167 (2000) 51.
10. P.V. Kamat, R. Huehn, R. Nicolaescu, *J. Phys. Chem.*, 106 (2002) 788.
11. M.R. Hoffmann, S.T. Martin, W. Choi, D.W. Bahnemann, *Chem. Rev.* 95(1995) 69.
12. E. Carpio, P. Zuniga, S. Ponce, J. Solis, J. Rodriguez, *J. Mol. Catal. A: Chem.*, 228 (2005) 293.
13. N. Serpone and E. Pelizzetti, *Photocatalysis, Fundamentals and Applications*, John Willey & Sons, N.Y (1989).
14. C. Kormann, D.W. Bahnemann, M.R. Hoffmann, *Environ. Sci. Technol.*, 25(1991) 494.
15. G. Palmisano, M. Addamo, V. Augugliaro, T. Caronna, A. Di Paola, E.G. Lopez, V. Loddo, G. Marci, L. Palmesano, M. Schiavello, *Catal. Today*, 122 (2007) 118.
16. H. Ogawa, *J. Phys. Org. Chem.*, 4 (1991) 346.
17. M. Hügül, I. Boz, R. Apak, *J. Hazard. Mater.*, 64 (1999) 313.
18. H. S. Wahab, T. Bredow, S. M. Aliwi, *J. Mol. Struct.*, 863(2008) 84.
19. T. Bredow and K. Jug, *Theor. Chem. Acc.* 113(2005) 1.
20. M.M. Ba-Abbad, A. A. Kadhum, A. B. Mohamad, M. S. Takriff, K. Sopian, *Int. J. Electrochem. Sci.*, 7(2012) 4871.
21. K.W. Al-Janabi, F.N. Alazawi, M.I. Mohammed, A.A. Kadhum, A. B. Mohamad, *Bull. Environ. Contam. Toxicol.*, 87(2011) 106.
22. E. H. El Ashry, A. El Nemr, S. A. Esawy, S. Ragab, *Electrochim. Acta*, 51 (2006) 3957.
23. E.E. Ebenso, D.A. Isabirye, N.O. Eddy, *Int. J. Mol. Sci.*, 11 (2010) 2473.
24. K. F. Khaled, *J. Solid State Electrochem.* 13 (2009) 1743.
25. H. S. Wahab, T. Bredow, S.M. Aliwi, *J. Mol. Struct.*, 863(2008) 84.

26. J. Bandara, J.A. Mielczarski, A. Lopez, J. Kiwi, *Appl. Catal.*, B, 34 (2001) 321.
27. J.M. Mercero, J.M. Matxain, X. Lopez, D.M. York, A. Largo, L.A. Eriksson, J.M. Ugalde, *Int. J. Mass spectrom.*, 240 (2005) 37.
28. G. Gece, *Corros. Sci.*, 50 (2008) 2981.
29. E. G. Lewars, *Computational chemistry: introduction to the theory and applications of molecular and quantum mechanics*. Second edition, Springer, New York (2000).
30. A. R. Katritzky, C. A. Ramsden, J. A. Joule, V. V. Zhdankin, *Handbook of Heterocyclic Chemistry*. Third edition, Elsevier, Netherland (2010).
31. M. Özcan, İ. Dehri, M. Erbil, *Appl. Surf. Sci.*, 236 (2004) 155.
32. E. E. Ebenso and I. B. Obot, *Int. J. Electrochem. Sci.*, 5(2010) 2012.
33. S.M. Quraishi, M.A. Quraishi, R. Quraishi, *The Open Corros. J.* 2(2009) 83-87.
34. A. Y. Musa, M. M. Ba-Abbad, A. A. Kadhum, A. B. Mohamad, *Res. Chem. Intermed.* 38 (2011) 995.
35. J. Suegara, B. D. Lee, M. P. Espino, S. Nakai, M. Hosomi, *Chemosphere*, 61(2005) 341.
36. B. Tan, X. Long, R. Peng, H. Li, B. Jin, S. Chu, H. Dong, *J. Hazard. Mater.*, 183 (2010) 908.
37. D.S. Bhatkhande, S.B. Sawant, J.C. Schouten, V.G. Pangarkar. *J. Chem. Technol. Biotechnol.* 79 (2004) 354.
38. X. Li, J.W. Cubbage, W.S. Jenks, *J. Org. Chem.*, 64(1999) 8525.
39. X. Li, J.W. Cubbage, T.A. Tetzlaff, W.S. Jenks, *J. Org. Chem.*, 64 (1999.)8509.
40. D.E. Park, J.L. Zhang, K. Ikeue, H. Yamashita, M. Anpo, *J. Catal.*, 185(1999) 114.
41. V. Subramanian, V.G. Pangarkar, A.A. Beenackers, *Clean Technol. Environ. Policy*, 2(2000) 149.
42. K. Tanaka, K. Padarmpole, T. Hisanaga, *Water Res.*, 34 (2000)327.
43. M.A. Fox, M.T. Dulay, *Chem. Rev.*, 93(1993) 341.